

УДК 539.1.08

CALIBRATION OF SPES4- π SET-UP IN EXPERIMENTS ON SATURNE-II

L.V. Malinina, E.A. Strokovsky

Calibration and alignment of the SPES4- π set-up components are described. The procedure is verified using real data on the elastic backward (in c.m.) $p(d, p)d$ scattering taken in the course of the experiment on study of inelastic (d, d') scattering of protons with excitation of $N(1440)$ and Δ -isobar.

The investigation has been performed at the Laboratory of High Energies, JINR.

Калибровка спектрометра SPES4- π в экспериментах на ускорителе SATURNE-II

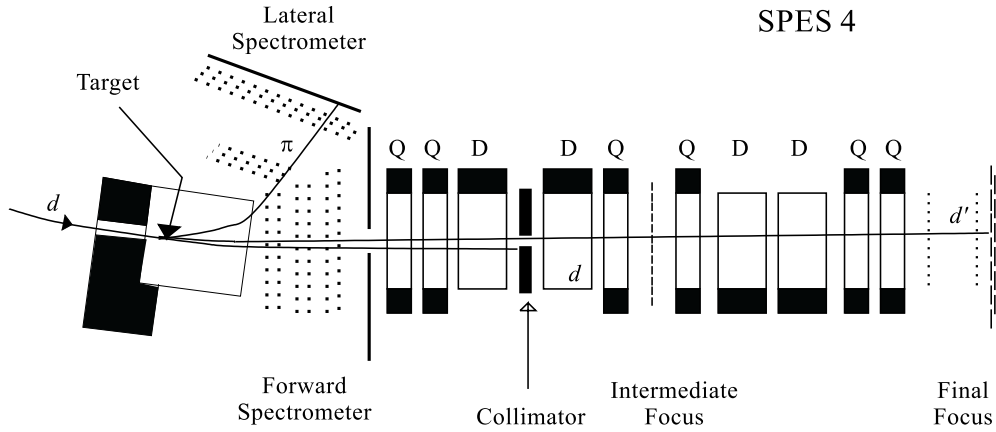
Л.В. Малинина, Е.А. Строковский

Рассматриваются процедуры калибровки и геометрического выстраивания частей спектрометра SPES4- π . Проверка правильности описанных процедур осуществлялась с помощью данных о реакции упругого $p(d, p)d$ рассеяния назад в системе центра масс, полученных в процессе проведения эксперимента по изучению неупругого (d, d') рассеяния протонов с возбуждением $N(1440)$ и Δ -изобар.

Работа выполнена в Лаборатории высоких энергий ОИЯИ.

INTRODUCTION

With the goal of exclusive study of the lowest baryon resonances excitation, in particular the Roper $N(1440)$ MeV, in the interactions of α particles and polarized deuterons with protons, the high resolution focusing spectrometer SPES-4 [1] at SATURNE II has been equipped with a two-arm detection system working in coincidence with it (Fig. 1). This system includes a dipole magnet, TETHYS, a 6cm liquid hydrogen target placed in the median plane of the magnet and two wide-aperture spectrometers (Forward, FS, and Lateral, LS) consisting of proportional (LS) and drift (FS) chambers and scintillation hodoscopes used for triggering and particle identification. The particles of high momenta (α' or d') scattered at small angle were detected in SPES-4 while the charged secondaries of significantly lower momenta (protons, pions, deuterons) were detected in the non-focusing spectrometer «FS+LS». Description of the Forward Spectrometer is given in Ref. 2; see also Refs. 3, 4. In this paper the calibration and alignment of FS and SPES-4 subsystems of the SPES4- π set-up are considered.

Fig. 1. Schematic view of SPES-4 π set-up

The paper is organized as follows. Calibration and alignment of the Forward Spectrometer components are described in the 1st chapter. Calibration of SPES-4 spectrometer with only scintillation hodoscope in its focal plane is considered in the second chapter. Verification of the calibration procedure is described in the concluding chapter using data on elastic backward (in c.m.) $p(d, p)d$ scattering with recoil protons detected by SPES-4 in coincidence with scattered deuterons detected in the Forward Spectrometer.

1. FORWARD SPECTROMETER ALIGNMENT PROCEDURE

The FS drift chamber assembly includes 6 chambers (X1, Y1, U, V, Y2, X2). Each chamber of FS had a «hole» free from the sensitive wires approximately in the middle of the chamber plane. The intensive primary beam of deuterons or α particles (and forward scattered projectiles or other reaction products) passed through the hole which divides a chamber to the right and left (X1, X2, U, V) or top and bottom (Y1, Y2) independent parts: the half-planes. The alignment procedure was done for the half-planes including verification of the «hole» actual sizes.

The following **coordinate system** was used (Fig. 2) in the data treatment: Z axis is directed along with the normal to the X1 plane, the axis X is parallel to the X1 plane and is directed as is shown on the Figure, Y axis is directed upward so as to form right-handed coordinate system. The origin of the Global Coordinate System was fixed at the centre of the hole of the first chamber X1 (the point L).

In the momentum reconstruction procedure [4] the x_1, x_2, y_1, y_2 coordinates were used to obtain for each particle emitted from the target its momentum (p), horizontal (θ_x) and vertical (θ_y) emission angles; z coordinate of the interaction point was fixed at the target centre (this assumption results in an uncertainty of the reconstructed momentum and gives one of the main contributions to the momentum resolution of the FS spectrometer).

The position of the origin of the Global Coordinate System (the point L) relative to TETHYS poles was calculated using the coordinates of the reference points which determine the optical axis of SPES-4. These coordinates had been specially measured at LNS using

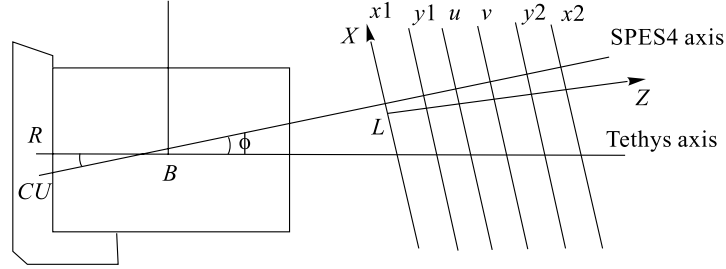


Fig. 2. Definition of the Global Coordinate System

geodesical methods. The accuracy of these measurements was ~ 0.5 mm. The positions of the other chambers X2, U, V, Y1, Y2 relative to X1 were measured with worse accuracy of ~ 2 mm.

1.1. Coordinate Measurements in the Forward Spectrometer Drift Chambers. Each plane of the FS chambers has two layers of the signal (anode) wires surrounded by cathode wires. The cathode wires formed the wall-less hexagonal structure (Fig 3). A charged particle crossing a chamber produces a signal in neighbours anodes.

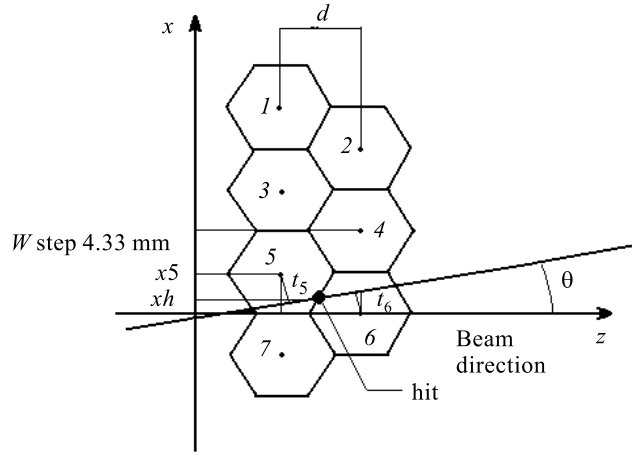


Fig. 3. Drift-cells structure of the FS

When the angle θ between the particle trajectory and the normal to the chamber plane is small, two neighbour anodes produced a signal (Fig 3). When the angle is large, it is possible that three (or more) neighbour wires produce the signal.

Let a particle crosses the chamber plane at angle θ and produces the signals on two neighbour wires x_i and x_{i+1} (in Fig. 3, $i = 5$). Then the coordinate x_h of the intersection of the particle trajectory with the chamber plane can be determined as

$$x_h = x_i - \frac{t_i * v_d}{\cos(\theta)} + \frac{d}{2 * \tan(\theta)}$$

$$x_h = x_{i+1} + \frac{t_{i+1} * v_d}{\cos(\theta)} - \frac{d}{2 * \text{tg}(\theta)}$$

where v_d is the experimentally measured electron drift velocity [3] ($v_d \simeq 50$ mkm/ns), d is the distance between two rows of the anode wires (Fig 3). Then

$$x_h = \frac{(x_{i+1} + x_i)}{2} + \frac{(t_{i+1} - t_i) * v_d}{2 * \cos(\theta)} .$$

In the data treatment the approximate formula was used (the angle θ was rather small and therefore was neglected):

$$x_h = \frac{(x_{i+1} + x_i)}{2} + a * (N_{i+1} - N_i), \quad (1)$$

where N_i is the «number of the time-slice» (see Ref. 3), corresponding to t_i ; a is the constant of about ~ 0.45 mm: this constant relates the N_i with the electron drift path per one time-slice:

$$2a = 50 \text{ (mkm/ns)} * 18 \text{ (ns)} = 0.9 \text{ (mm)}.$$

The eq. (1) was used to calculate coordinates in all the chambers X1, X2, Y1, Y2, U, V. Neglecting the drift time information results in eq. (1'):

$$x_h = \frac{(x_{i+1} + x_i)}{2} \quad (1')$$

used in the «proportional chamber» mode of the coordinate measurements.

1.2. Alignment Procedure of the Chambers of the Forward Spectrometer (YZ-Plane).

The procedure of the alignment in YZ plane preceded the procedure of alignment of chambers with inclined wires (U,V), because the latter needs information about y -coordinates (see Sect. 3).

As it was done for the case of run with α particle beam (see Ref.5), alignment of Y-chambers relative to the median plane of TETHYS was based on two experimental facts: 1) the target was placed in the median plane of the magnet (i.e., its centre was placed at $y = 0$); 2) the magnetic field is symmetrical in Y direction relative to the median plane (below it is called «up-down symmetry») which is, by definition, the XZ plane of the coordinate system.

It was impossible to use the same sample of the calibration data (straight lines, magnetic field switched off) as it was for XZ alignment (see below, subsection. 1.3), because in that sample the beam was too wide in the target region (± 5 cm) and passed throughout the target mostly without scattering. Therefore to perform alignment of Y chambers, a part of real experimental data on $(d, d')X$ scattering with at least one charged particle with momentum in the interval of 0.6–1.1 GeV/c in FS was used. The data were taken at magnetic field of TETHYS of 0.8142 tesla.

The idea of the method is the following: because the target centre was located in the median plane of TETHYS, (i.e. at $y = 0$), the Y projections of tracks of all scattered particles emitted from the target with momenta indicated above must cross the median plane of the magnet in the vicinity of the target region and the Y projections of envelopes of tracks hitting top and bottom parts of the Y chambers must be symmetric relative to the same plane due to the up-down symmetry of the field. Obviously, because of presence of B_x, B_z components

of the fringe magnetic field (the map of the field is described in detail elsewhere [4]), the mean z coordinate of the crossing point should not necessarily coincide with the target centre coordinate. (Actually, it is displaced on about of ~ 3 cm upstream of the target centre.) This is seen on Fig. 4 for simulated events with momenta of 0.6–1.1 GeV/c traced through the TETHYS magnetic field of 0.8142 T.

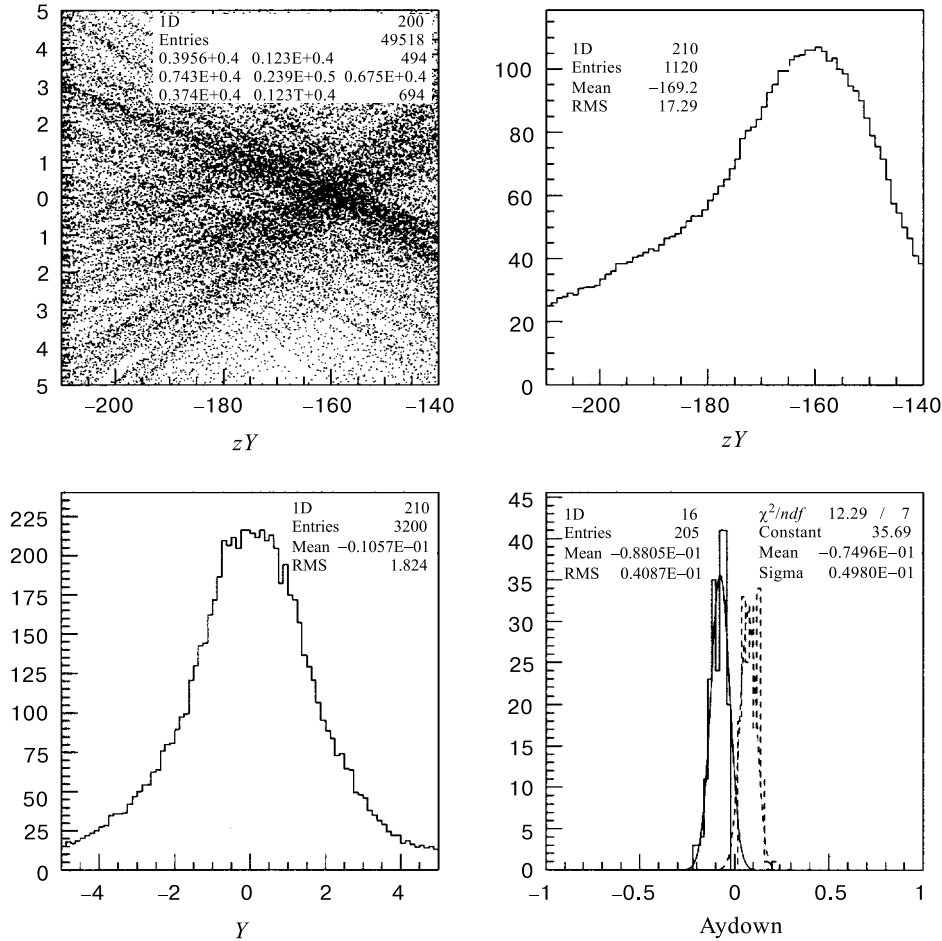


Fig. 4. Monte-Carlo simulated events (secondaries with momenta of 0.6–1.1 GeV/c) traced through the set-up at TETHYS magnetic field of 0.8142 T. Top left (1): tracks crossing top and bottom parts of Y traced back. Axii: z coordinate in the Global Coordinate System (GCS) — abscissa, y coordinate (in the GCS) — ordinate. Top right: projection of the bidimensional distribution (1) onto the abscissa axis, i.e., distribution on z coordinate of the emission point. Bottom left: projection of the bidimensional plot (1) on the ordinate, i.e., the distribution on y coordinate of the emission point. Bottom right: the mismatches for the vertical emission angle

In the analysis, particles with tracks crossing top and bottom parts of the Y chambers were treated separately. For each particle its track was traced back and the functional

$$a_y * z_t + b_y \rightarrow 0.$$

was minimized to obtain the point z_t of intersection with median plane (where y coordinate is zero). Here:

$$a_y = (y_2 + \delta y_2 - (y_1 + \delta y_1)) / (z_{Y1} - z_{Y2}), \quad (2a)$$

$$b_y = (y_1 + \delta y_1) - a_y * z_{Y1} \quad (2b)$$

free parameters are: Y chamber offsets δy_1 , δy_2 and the intersection coordinate z_t .

In the experimental data the point of intersection of the tracks hitting top and bottom parts of the Y chambers did not appear in the median plane when δy_1 and δy_2 are set to zero «by hand» (Fig. 5).

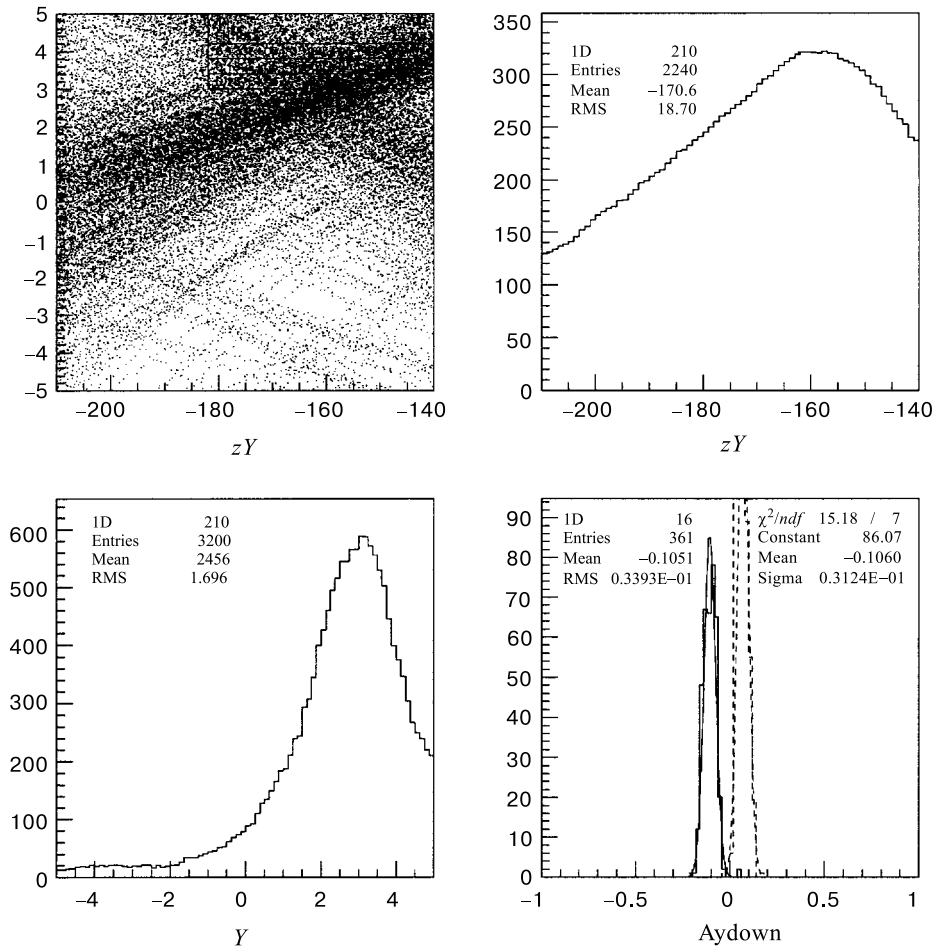


Fig. 5. The same as on the previous figure but for real events from $p(d, d')X$ scattering with secondaries at momenta of 0.6–1.1 GeV/c (TETHYS magnetic field is 0.8142 T); before Y alignment

The result of minimization is as follows:

$$\delta y1 = 0.324 \pm 0.104 \text{ cm}$$

$$\delta y2 = -0.306 \pm 0.127 \text{ cm}$$

$$\langle z_t \rangle = -158. \pm 0.03 \text{ cm}$$

with $\chi^2/dof \sim 0.32$

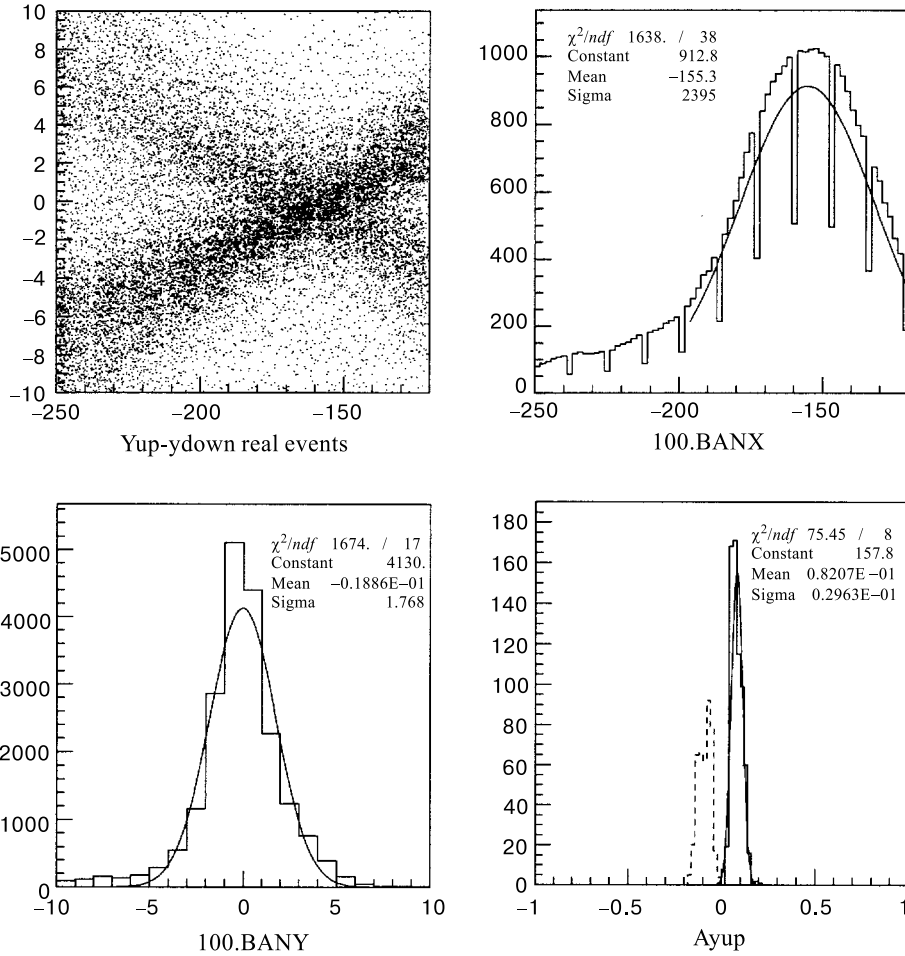


Fig. 6. The same as in the previous figure: after Y alignment

Figure 6 represents the real data when y coordinates are corrected: the point of intersection of the tracks with z axis is in the median plane, the mean $\langle z_t \rangle$ value is close to the mean z coordinate of this point calculated by Monte Carlo (Fig. 4) for $B=0.8142$ T and $p = 0.6 - 1.1$ GeV/c.

1.3. Alignment of the Chambers of the Forward Spectrometer in XZ-Plane.

1.3.1. Verification of X1, X2 chamber positions relative to the Global Coordinate System.

To verify the position of X1, X2 chambers relative to TETHYS magnet, the events of the well identified process $dp \rightarrow pd$ [4] in the sample of real data were selected. For these events with known type of the particles (d) detected in FS, the momentum, the horizontal (θ_x) and vertical ($\theta_y \sim 0$) scattering angles have been found using the momentum reconstruction procedure [4]. Distributions on the reconstructed scattering angle (θ_x) and momentum of the backward (in c.m.) scattered deuterons are shown in Fig. 7. It is seen that the reconstructed momentum

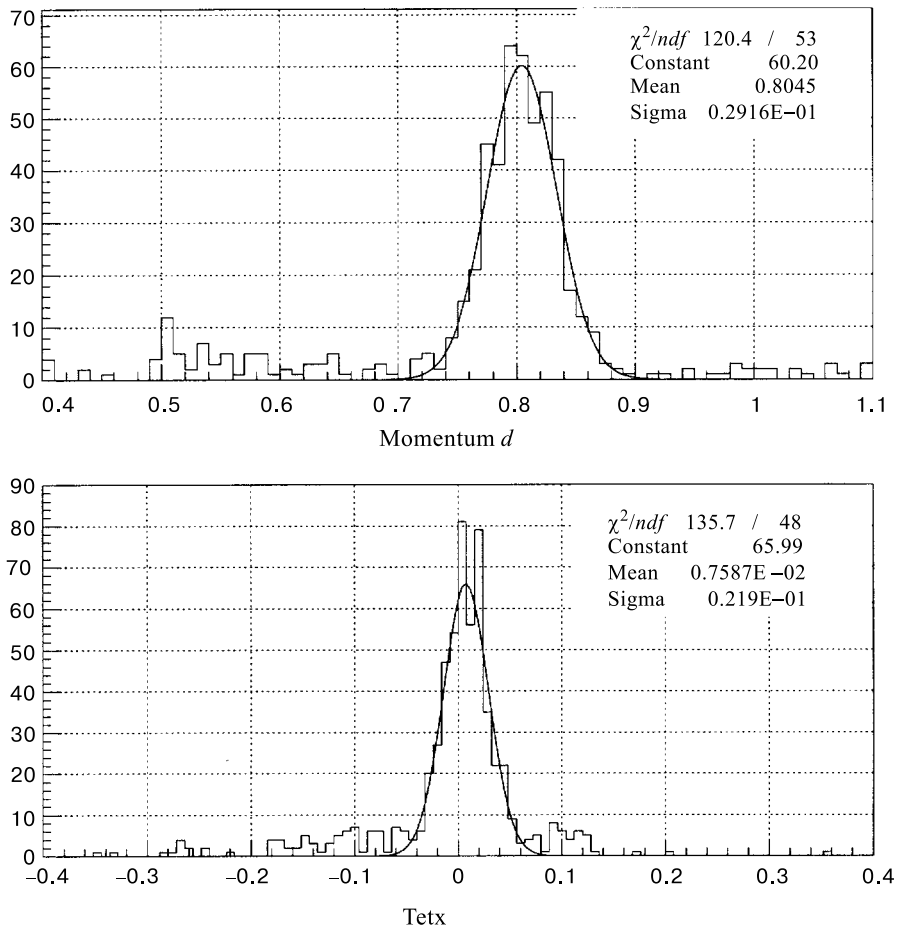


Fig. 7. Momentum and the emission angle of deuterons from $dp \rightarrow pd$ at 180° at c.m.; here the «proportional chamber mode» was used for tracking

$P_d = 0.805 \pm 0.002$ GeV/c and the scattering angle $\theta_x = 0.008 \pm 0.001$ rad are in good agreement with those expected from the $p + d \rightarrow d + p$ kinematics at the beam momentum $p_d = 3.73$ GeV/c. The widths of the momentum and the angular distributions are determined

by the uncertainty in the z coordinate of the interaction point, multiple Coulomb scattering in air and in the material of the target and its surrounding, material of the drift chambers, the accuracy of measurements of the coordinates and the accuracy of the measurements and extrapolation procedures of the magnetic field map. (The method used here and described in Ref. 4, differs from that described in Refs. 2, 3, but gives practically the same results being applied to the same data set.)

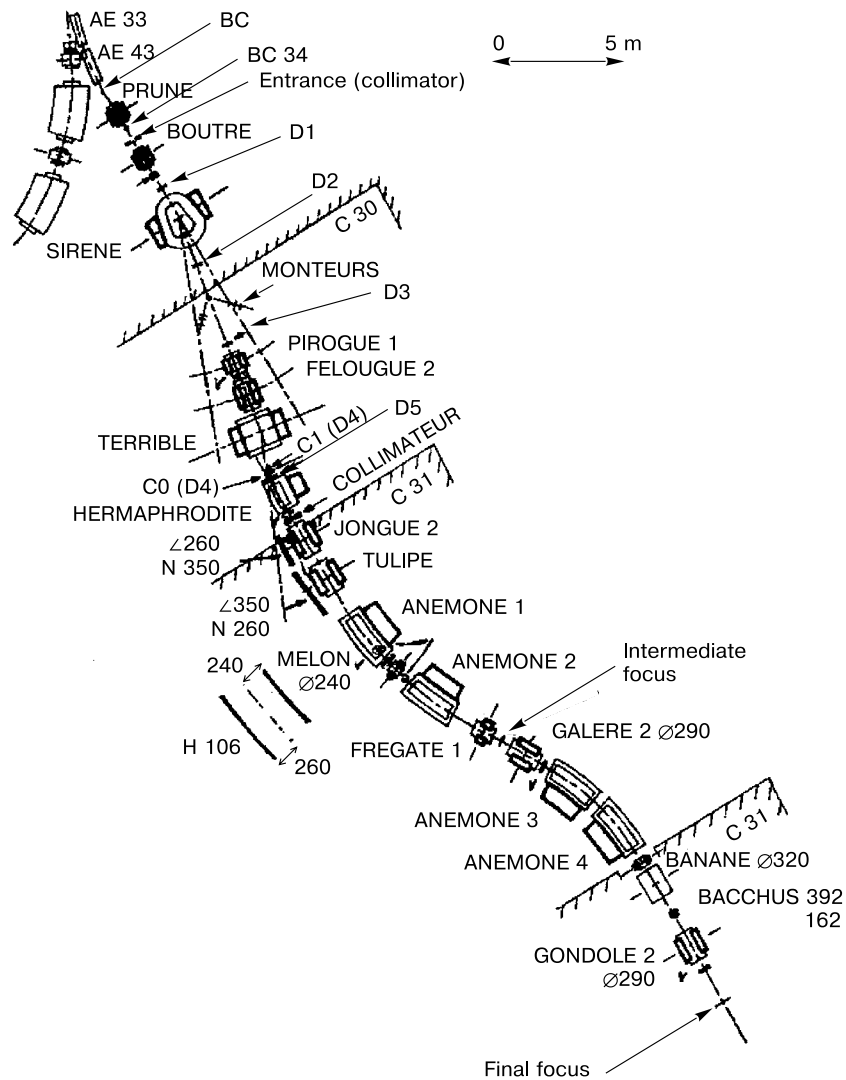


Fig. 8. SPES-4 beam line at SATURNE-II (before the rearrangement of the D5 area, where TETHYS magnet surrounded by FS and LS was installed instead of HERMAPHRODITE dipole). Beam intensity was defined by opening the collimator as indicated in the Figure

A displacement of ~ 2 cm in the X1, X2 chambers X-positions relative to TETHYS magnet or an error in the position of X2 relative to X1 of ~ 0.6 cm ($10 \text{ mrad} \times 60.6 \text{ cm}$) results in the shift of the mean momentum of deuterons from the elastic backward scattering $dp \rightarrow pd$ of $\sim 30 \text{ MeV}/c$; therefore if the measured value of the deuteron momentum were shifted out on a value of one standard deviation from the correct value, the error of the geometrical measurements of relative X1, X2 positions should have been much more than ~ 6 mm or the error of the position of X1, X2 relative to TETHYS should have been much more than 2 cm. (Note that the accuracy of the geometrical measurements in this experiment was not worse than ≤ 2 mm.)

1.3.2. Alignment of the chambers with inclined wires. The alignment of U, V chambers relative to X1, X2 chambers was done using data taken with the direct deuteron beam of low intensity. The low intensity ($\sim 10^8$) beam in this experiment was prepared as follows: the extracted beam of high intensity was defocused before the 1st collimator of the beam line (see Fig. 8); intensity of the beam after the collimator was determined by its opening. In these measurements, TETHYS magnet was switched off so that rectilinear tracks passing from the target to the FS hodoscope were recorded. The data were taken with a simple trigger initiated by a signal from one of the counters of the FS scintillation hodoscope.

The U and V chambers had their wires inclined in opposite directions by the angle $\sim \pm 10^0$ with respect to the wire direction of the X chambers.

These chambers have been used to link the Y and X projections of the track in the case when more than one track was detected in the FS. The x coordinates of the particles in U and V chambers (x_u, x_v) are calculated (as is shown in Fig. 9, where the angle θ_u is defined as positive; and θ_v , as negative) from the measured coordinates u, v and y_1, y_2 : (a_y and b_y are defined in Eqs. (2)):

$$x_u = \frac{u}{\cos(\theta_u)} + y_u * \tg(\theta_u); \quad y_u = a_y \cdot z_u + b_y, \quad (3)$$

$$x_v = \frac{v}{\cos(\theta_v)} + y_v * \tg(\theta_v); \quad y_v = a_y \cdot z_v + b_y. \quad (4)$$

(Here $z_u, (z_v)$ are the z coordinates of the points of intersections of U, V chambers with the perpendicular to X1, X2 planes.) In the off-line data treatment the events which have only one «hit» in each chamber (X1, X2, U, V, Y1, Y2) have been chosen. The «hit» in this case means a group of two or three neighbour wires. The procedure of the calculation of centre of the «hit» using drift time information was described already in the subsec. 1.1.

The x_u, x_v coordinates can be calculated according to equations (3), (4) and also directly from the coordinates measured in X1, X2 chambers (x_1, x_2):

$$x_{ux1,x2} = a_x * z_u + b_x, \quad (5)$$

$$x_{vx1,x2} = a_x * z_v + b_x, \quad (6)$$

where a_x, b_x are the parameters of the straight line traced through x_1, x_2 . The main goal of the alignment procedure is to find such relative offsets between the chambers as well as the inclination angles of the wires of U and V chambers, which minimize the differences:

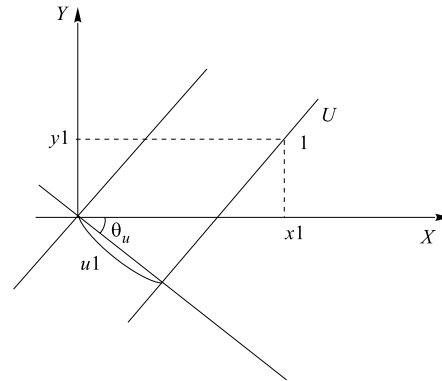


Fig. 9. Drawing to the x_u, x_v calculation

$$\Delta_{xu} = x_u - x_{ux1,x2}, \quad (7)$$

$$\Delta_{xv} = x_v - x_{vx1,x2}. \quad (8)$$

The minimization of the functionals

$$var1 = \left(\frac{u}{\cos(\theta_u)} + y_u * tg(\theta_u) + \delta_{xu} - x_u \right)^2, \quad (9)$$

$$var2 = \left(\frac{v}{\cos(\theta_v)} - y_v * tg(\theta_v) + \delta_{xv} - x_v \right)^2 \quad (10)$$

has been done using the inclination angles θ_u, θ_v and the offsets of the U, V chambers along the x direction (d_{xu}, d_{xv}) as the free parameters.

The minimization has been done for right parts of U and V chambers because of the direct defocused beam position. The results are presented in the Table and Fig. 10.

Table. Offsets δ_u, δ_v and inclination angles θ_u, θ_v

	U	V
χ^2/dof	~ 1.39	~ 1.22
$\delta_{xu}(v)$ (cm)	0.372 ± 0.002	0.246 ± 0.002
θ_u (θ_v) (degree)	9.55 ± 0.01	-9.73 ± 0.01

Expected [3, 5] coordinate resolution of the FS is of ~ 0.3 mm in the «drift mode»; the expected resolution for «proportional chamber mode» (when only wire numbers were used for tracking) is ~ 1.2 mm because the distance of the two neighbour drift cells is 4.33 mm. In Fig. 10 the distributions of Δ_{xu}, Δ_{xv} are shown for both modes: the «proportional chamber mode» (Fig. 10, top) and the «drift mode» with the best minimization parameters (Table) ($\sigma_{\Delta_{xu}} = 0.31$ mm, $\sigma_{\Delta_{xv}} = 0.33$ mm) (Fig. 10, bottom). Using these values, one can see that the intrinsic coordinate resolution of an individual chamber is as expected: $\sigma = 0.3$ mm.

2. SPES-4 TIME ALIGNMENT AND CALIBRATION

2.1. SPES-4 Spectrometer: an Outlook. SPES-4 spectrometer [1] (Fig. 8) is ~ 33 meter long and consists of two almost identical bends, made of four identical dipoles, six quadrupoles and a correcting sextupole. It has normally two detectors: the scintillation hodoscope placed at the intermediate focus (I , after the first bend) and the Focal Plane Detector (FPD) placed in the final focus (F). The FPD consists of the scintillation hodoscope (also denoted as F), 2 cm thick scintillators (ΔE -detector) placed after the F hodoscope in order to measure ionization losses of the detected particles and two drift chambers (with four wire planes each) before the F hodoscope. (In this experiment the drift chambers were not used in the measurements

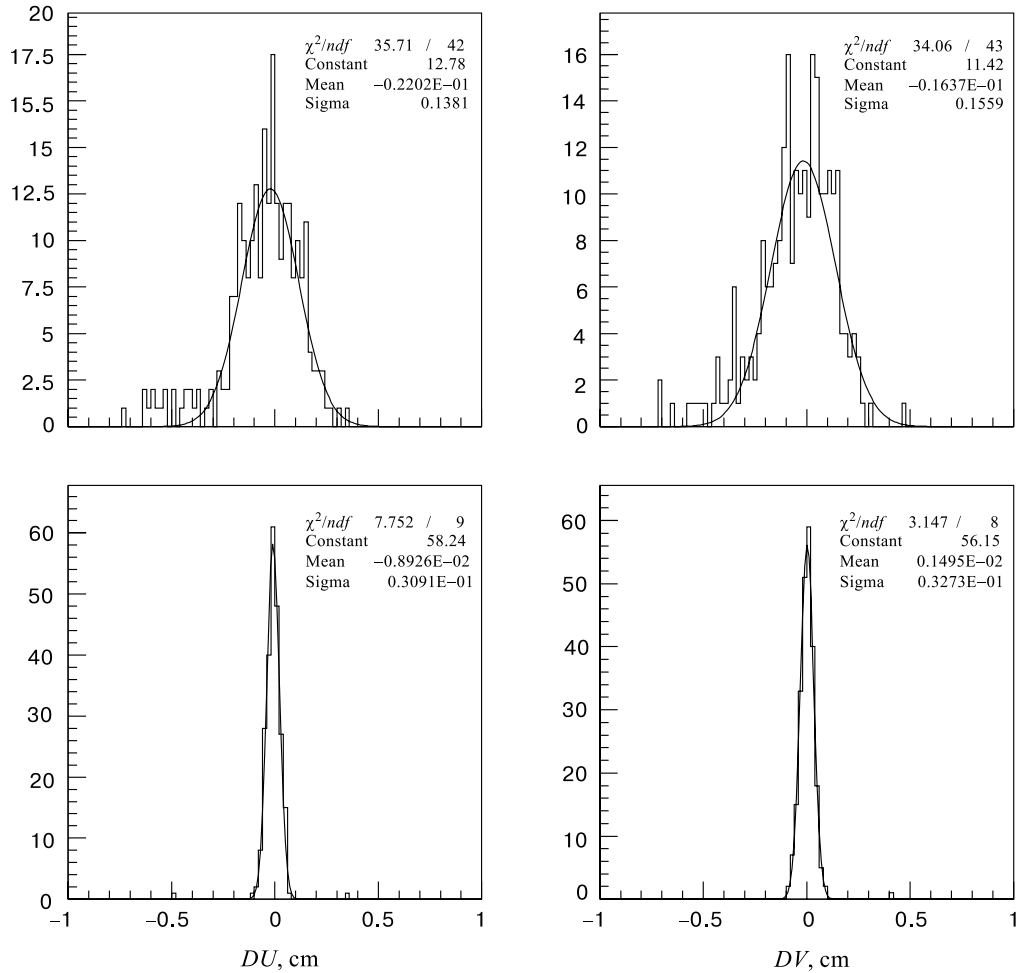


Fig. 10. The intrinsic resolution of the Forward Spectrometer chambers for the «proportional chamber» (top) and «drift chamber» modes (bottom)

most of the time.) Particles detected in SPES-4 are identified usually by the values of p/z , time of flight between I and F hodoscopes and the energy deposit in the ΔE -detector*.

In this experiment only single charged particles were detected (protons or deuterons). Therefore the same method as described in Ref. 1 was used for particle identification. It is based mostly on the information about time-of-flight and momentum of the detected particle: its mass M_{det} was calculated as described in subsection 2.3 and corresponding cuts were applied.

The hodoscope in the intermediate plane (I) consisted of 12 scintillation counters; the focal plane hodoscope F actually consisted of two hodoscopes ($F1$ and $F2$) from 12 and 13

*Here p is the momentum of the detected particle; z , its charge.

counters respectively. The neighbour counters of the F detector, F_i and F_{i+1} , overlap each other in such a way that the distance between their centres was equal to the half of the width of the individual counter. The Focal Plane Detector provided FPD signal for the full trigger of SPES4- π set-up. The FPD signal was organized in such a way that only coincidence combinations of $[(I_i \wedge F_i) \vee (I_i \wedge F_{i+1}) \vee (I_i \wedge (F_i \wedge F_{i+1}))]$ were allowed. (Note that the combination $[(I_i \wedge F_{i+1}) \vee (I_i \wedge (F_i \wedge F_{i+1}))]$ is the most probable for all the counters but the 1st and the last ones in the F hodoscope.)

In this experiment only small sample of the data was taken using the drift chambers of the SPES-4 Focal Plane Detector. This sample was used for calibration of the F hodoscope, i.e., in order to determine a function which relates momentum of particles detected by the F_i counter with the counter number i : $\Delta p_i/p_0 = (p_i - p_0)/p_0 = f(i)$. Here p_0 is the «central» momentum of SPES-4: particles of this momentum remain on the spectrometer axis if they entered the spectrometer at the axis and parallel to it.

It is well known that the SPES-4 acceptance (for a point-like source placed at its axis at the same distance from the entrance window of the spectrometer as the target used in the experiment) is characterized by the $\Delta p/p_0$ and two angles (vertical, Θ_y and horizontal, Θ_x) between the spectrometer axis and the track of a particle emitted from the source. The acceptance on Θ_y does depend upon $\Delta p/p_0$ and was about of ± 5.8 mrad. The boundaries for accepted values of $\Delta p/p_0$ and Θ_x are correlated; only particles emitted by the point-like source with $\Delta p/p_0$ and Θ_x inside the region shown in Fig. 11 can be detected by the spectrometer. This region is inside the rectangular $|\Delta p/p_0| \sim 5\%$ and $|\Theta_x| \sim 15$ mrad. Using only F -hodoscopes one gets the typical momentum bin width of $\sim 0.8\%$; inside each of the momentum bin an integration over Θ_x is performed by the set-up (see Fig. 11).

The procedure of the SPES-4 calibration included the following steps:

1. Time alignment of the I and F individual counters using the sample of data with all three counters fired: $I_i \wedge (F_i \wedge F_{i+1})$;
2. The calibration of SPES-4: finding numerical values for linear form $f(i)$ in the relation

$$\Delta p_i/p_0 = (p_i - p_0)/p_0 = f(i) \quad .$$

3. Time re-alignment of the individual I and F counters taking into account that particles of different momenta have slightly different time of flight between I and F counters.
4. Verification of the calibration using data for the elastic backward (in c.m.) $p(d,p)d$ scattering: the recoil proton momentum measured in SPES-4 must be independent of the

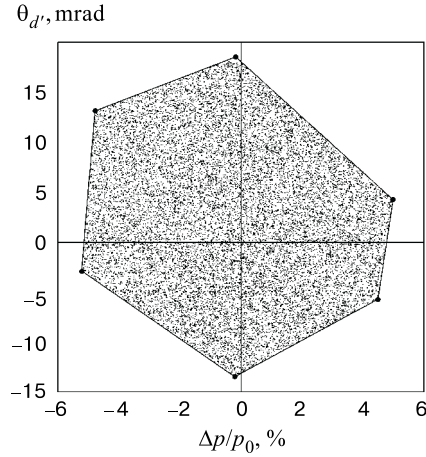


Fig. 11. The typical shape of the acceptance of SPES-4 on the plane $(\Delta p_i/p_0, \Theta_d')$ in this experiment. Here Θ_d' is the plane (horizontal) angle between SPES-4 optical axis and the scattered deuteron momentum direction at the entrance of SPES-4

SPES-4 tuning. After this the final check of the whole procedure was done by checking that mass of a particles detected in SPES-4 does not dependent upon the whole set-up setting and upon the particle momentum.

2.2. Calibration of SPES-4. Despite SPES-4 spectrometer was used in many experiments and its properties are well known, in this experiment only part of the full FPD was used. Therefore it was necessary to perform independent calibration of the instrument.

Most of the event detected in SPES-4 belong to the type of $[(I_i \wedge F_{i+1}) \vee (I_i \wedge (F_i \wedge F_{i+1}))]$. Therefore it is straightforward to find relative time offsets between neighbour F counters and the corresponding I counter. The only correction to be introduced is the correction for different time of flight between I and F planes for particles with different momenta but the same type (it is possible, in rather good approximation, to neglect the difference in flight paths for particles having different trajectories in SPES-4).

The time alignment was done using a special sample taken at such SPES4- π setting that almost all particles accepted by SPES-4 were deuterons; the set-up was triggered by FPD of SPES-4 only.

The same sample was used in order to relate number of the «fired» F_i counter with the coordinate of the point where the detected particle hits the counter. This coordinate was determined using data from the drift chambers of the FPD. It was found that the corresponding relation is linear with good accuracy; this allows one to find numerical coefficients in the relation $\Delta p_i/p_0 = (p_i - p_0)/p_0 = A_F + B_F \cdot i$ (see Fig. 12)*.

2.3. Verification of the SPES-4 Calibration Constants. Particle Identification in SPES-4. Having data with monochromatic, well collimated beam of particles of one specie in SPES-4 taken at different settings of the set-up, it would be easy to verify the calibration of the SPES-4 spectrometer. Fortunately, such data were taken as a by-product in the course of the experiment, because, together with $p(d, d')$ data with deuteron detected by SPES-4, a sample of data from $p(d, p)d$ reaction at 180° in the c.m. (BES) was recorded at 3 different settings also. The latter reaction is well defined kinematically, what provides the desirable «beam» of particles of known specie (protons) and well defined momentum (2.926 GeV/c at initial deuteron momentum of 3.73 GeV/c). This «beam» is well collimated because of the sharp angular dependence of the cross section for this reaction. The three settings were considerably overlapped due to the relatively big momentum acceptance of SPES-4. In particular, at one setting protons from BES were detected near the central F counter, while at two other settings these protons were detected at opposite edges of the F hodoscope. The reaction can be easily

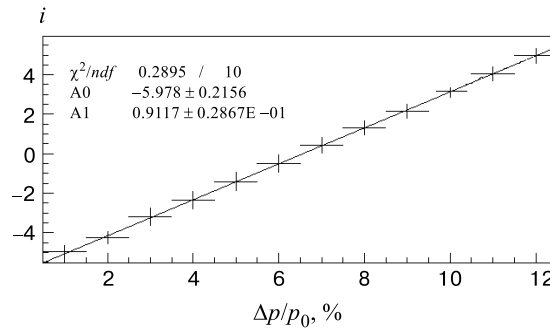


Fig. 12. Relation between $\Delta p/p_0$ (abscissa) and number i of the «fired» F counter

*The numerical values of the coefficients used in the subsequent analysis are: $A_F = -5.3325$, $B_F = 0.802$, when $\Delta p_i/p_0$ is taken in percent.

selected using information from the Forward Spectrometer (FS) scintillators. In addition, the recoil deuterons hit almost always only one of two of the FS counters.

All this allowed to verify the momentum calibration of SPES-4: if all the constants are correctly found, the momentum of the detected protons must be stable against changes of the settings and the data must be centered at momentum 2.926 GeV/c (the uncertainty in the peak position arises due to the relatively big width of the individual F counter). This check was done and it was found, that the stability is quite impressive.

1D	150	χ^2/ndf	1058. / 15	1D	150	χ^2/ndf	349.0/12
Entries	280183	Constant	.2239E+05 \pm 62.59	Entries	280464	Constant	1769. \pm 19.60
Mean	1.870	Mean	1.875 \pm 9663E-04	Mean	.9488	Mean	.9446 \pm .6149E-03
RMS	6215E-01	Sigma	.4138E-01 \pm .9200E-04	RMS	7610E-01	Sigma	.8772E-01 \pm .5828E-03

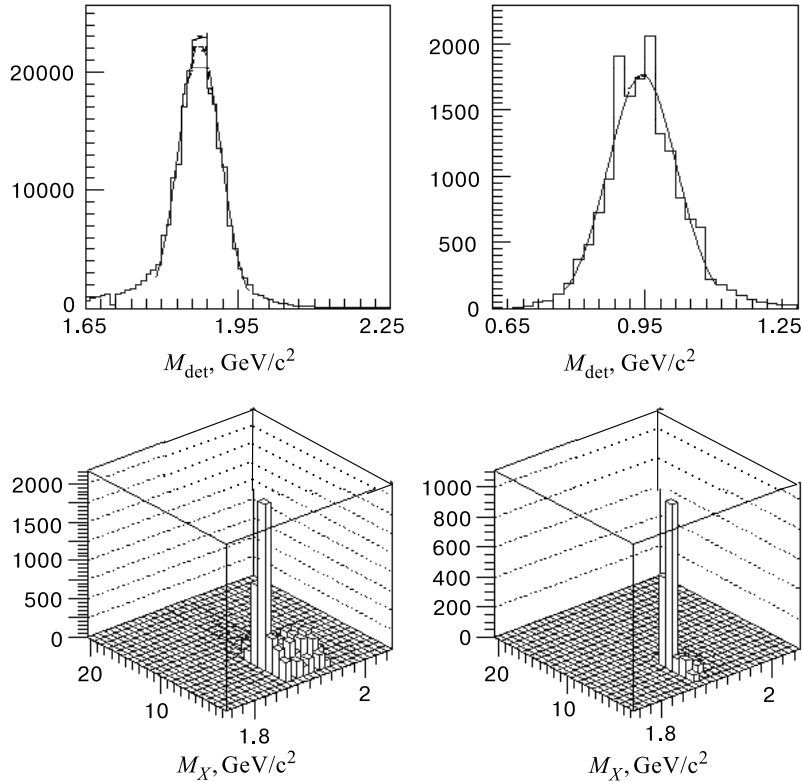


Fig. 13. Top left: mass of the deuterons measured in SPES-4. Top right: the same for particles identified as protons. Bottom left: missing mass M_X versus number of the first fired FS-counter. Here $M_X^2 = (P_{proj} - P_{eject})^2$ and P_{proj} is the 4-momentum of the projectile (deuteron), P_{eject} is the 4-momentum of the particle detected in SPES4. Bottom right: the same for events corresponding to the deuteron spot in the $tdc - adc$ spectrum measured in FS. (Here $tdc - adc$ spectrum represents distribution of the FS-events on the «time-of-flight versus energy deposit» plot.)

There exists another method to verify the SPES-4 calibration as well as to monitor the performance of the whole system including possible hardware drifts of the F and I detectors.

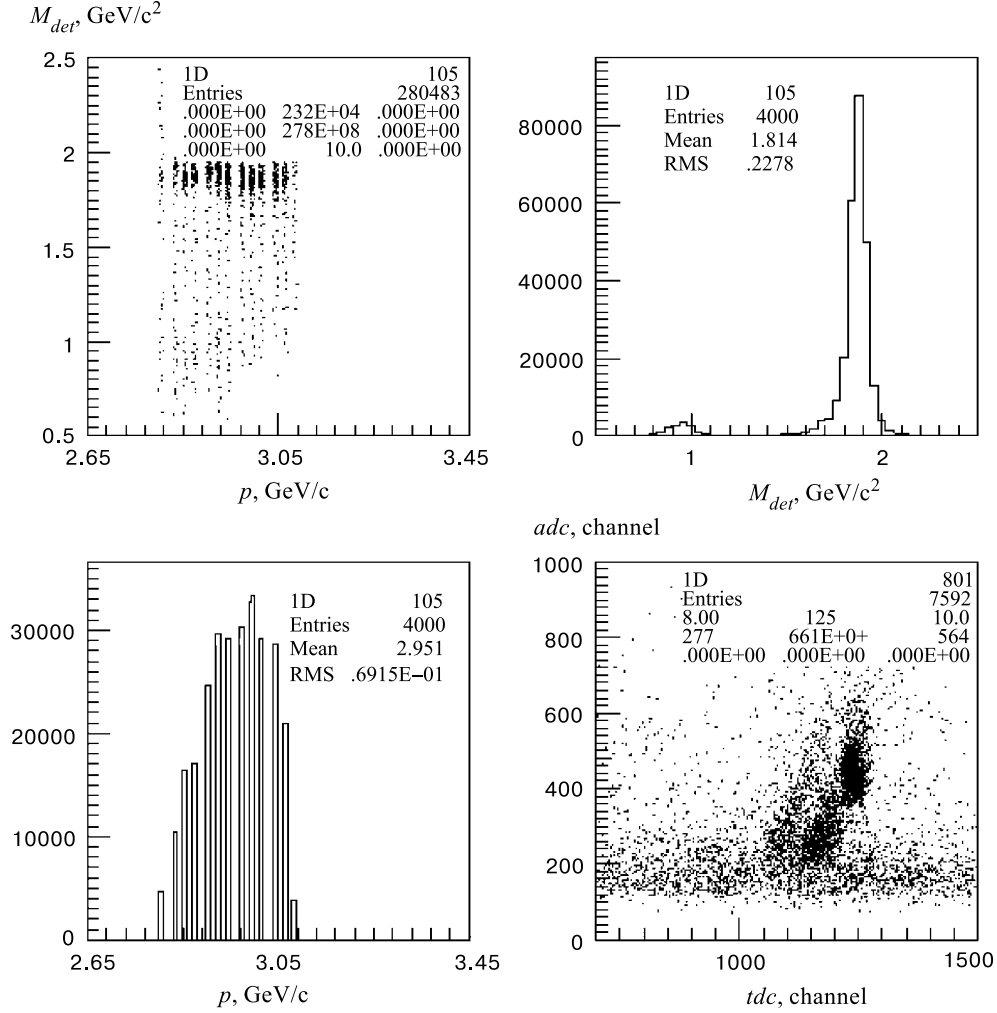


Fig. 14. Top left: mass of the particle detected in SPES-4 (ordinate) versus momentum of this particle (abscissa). Top right and bottom left: projections of this plot onto corresponding axes. Bottom left: $tdc - adc$ spectrum (see previous Figure) for identification of the BES channel (topmost-rightmost dark spot)

Any such drift influences «time of flight» values measured by these counters. Therefore monitoring of possible «jumps» and drifts is provided by monitoring of the value of mass of particle detected in SPES-4. The point is that the flight path L (of about 16.35 m) of any particle accepted by SPES-4 is almost independent of its momentum. Therefore, if the time of flight τ_{det} is measured correctly and the momentum of the detected particle p_{det} is also measured correctly, it is possible to calculate the mass M_{det} of the detected particle:

$$M_{det} = p_{det} \cdot \sqrt{\tau_{det} \cdot \frac{c}{L} - 1},$$

where c is the speed of light. The calculated value of M_{det} must be the same at all settings and must coincide (within the accuracy of the measurements) with tabulated mass of this particle. It is illustrated in Fig. 13 and Fig. 14: for deuterons in SPES-4 one gets $\langle M_{\text{det}} \rangle = 1.875 \pm 0.0001 \text{ GeV}/c^2$, for protons – $\langle M_{\text{det}} \rangle = 0.945 \pm 0.0001 \text{ GeV}/c^2$ respectively; resolution on the M_{det} is $\sigma_{M_{\text{det}}} \sim (40 \div 70) \text{ MeV}/c^2$.

The value of M_{det} was calculated for each detected particle and used for particle identification in SPES-4.

3. CONCLUSION

Procedure of alignment and calibration of SPES4- π set-up components (the Forward Spectrometer and SPES-4) is described. All constants defining the geometry of the set-up are found using specially taken data samples, part of the raw data and data on the elastic backward (in c.m.) $p(d, p)d$ scattering taken as a by-product in the course of the experiment. These $p(d, p)d$ data are interesting on its own and have been presented at European Few Body conference [4].

The procedure developed before for reconstruction of momentum and emission angle of particles detected in Forward Spectrometer was thoroughly checked. It is found to be adequate to the data of experiment 278 with SPES4- π set-up at SATURNE-II. The FS momentum resolution is found to be determined mostly by length of the hydrogen target and the method used for the momentum reconstruction.

Calibration of SPES-4 is done for the case when drift chambers of the standard FPD are not used. The method of particle identification described here and used in experiment of Ref.6 was applied to SPES-4 at first time.

The work was supported in part by INTAS-RFBR grant No.95-1345. We are grateful to L.S. Azhgirey for fruitful collaborative work in this experiment, G.D. Alkhazov, A.V. Kravtsov, A.N. Prokofiev, T. Hennino, R. Kunne, J.-L. Boyard for their interest to this work, fruitful and valuable discussions; to S.V. Kartashov and P.P. Korovin for their help and assistance in computing and to N.M. Piskunov, and V.V. Glagolev, A.A. Baldin and A.S. Vodopianov for their interest and support of this work.

References

1. Arvieux J. et al. — Phys. Rev. Lett., 1983, v.50, p.19;
Arvieux J. et al. — Nucl. Phys., 1984, v.A431, p.1613; Boudard A. — Thesis, CEA-N-2386, (1984) (unpublished).
2. Alkhazov G.D. et al. — Preprint PNPI EP-9-2000 No. 2352, PNPI, Gatchina, (2000).
3. Alkhazov G.D., Kravtsov A.V., Prokofiev A.N. — Preprint PNPI EP-32-1998 No. 2246, PNPI, Gatchina, (1998).
4. Azhgirey L.S. et al. — JINR Rapid Comm., 1999, 2[94]-99, p. 5. See also: Prokofiev A.N. et al. — In: Proceedings of the 16th European Conference on Few Body Problems in

- Physics, Autrans, France, June 1-6, 1998; ed. by B. Desplanques, Protasov K., Silvestre-Brac B., Carbonell J. — *Few Body Systems*, Suppl. 10, p.491;
Stokovsky E.A. et al. — *ibid*, p. 495.
5. Alkhazov G.D., Kravtsov A.V., Prokofiev A.N. — Preprint PNPI EP-27-1999 No. 2312, PNPI, Gatchina, (1999).
 6. Azhgirey L.S. et al. — *YaF*, 1998, v.61, p.494 (*Phys. At. Nucl.*, 1998, v.61, p. 432).

Received on June 15, 2000.